arXiv:1402.2748v3 [gr-qc] 10 Oct 2014

Regular Black Holes as Particle Accelerators

Parthapratim Pradhan[1]

Department of Physics
Vivekananda Satabarshiki Mahavidyalaya
Manikpara, West Midnapur
West Bengal 721513, India

Abstract

We investigate the possibility of arbitrarily high energy in the center of mass(CM) frame of colliding particles in the vicinity of the infinite red-shift surface of the spherically symmetric, static charged regular black holes (Bardeen black hole, Ayón-Beato and García black hole, and Hayward black hole). We show that the CM energy of colliding particles near the infinite red-shift surface of the *extreme* regular black holes are arbitrarily large while the non-extreme regular black holes have the finite energy. We also compute the equation of innermost stable circular orbit(ISCO), marginally bound circular orbit(MBCO) and circular photon orbit(CPO) of the above regular black holes, which are most relevant to black hole accretion disk theory.

1 Introduction

Recently, Bañados, Silk and West(hereafter BSW) [1] demonstrated that particles falling freely from rest exterior of a rotating extremal black hole can produce an infinite amount of high CM energy. In a semi-realistic setup, this energy could be higher than the Planckian energy, so that one might think extremal black hole could be act as super high energy particle accelerator. Soon the appearance of this work in the literature several practical objections to the proposed mechanism has been raised. Particularly in [2], the authors have shown that there is an astrophysical bound i.e. maximal spin, back reaction effect and gravitational radiation etc. on that CM energy due to the Thorn's bound [3] i.e. $a = 0.998M$ (M is the mass and $a = \frac{J}{M}$ is the angular momentum per unit mass of the black hole or Kerr parameter). Also Jacobson et al. [4] showed that CM energy in the near extremal situation for Kerr black hole is $\frac{E_{cm}}{2m_0} \sim \frac{2.41}{(1-a)^{1/4}}$. Lake [5] found that the CM energy at the inner horizon of a static Reissner-Nordstrøm(RN) black hole and Kerr black holes are limited. Grib et al. [6] investigated the CM energy using the multiple

[1]E-mail: ppradhan77@gmail.com

scattering mechanism. Also in [7], the same authors computed the CM energy of particle collisions in the ergo-sphere of the Kerr black hole. The collision in the ISCO particles was investigated by the Harada et al. [8] for Kerr black hole. Liu et al. [9] studied the BSW effect for Kerr-Taub-NUT(Newman, Unti, Tamburino) space-time and proved that the CM energy depends upon both the Kerr parameter (a) and the NUT parameter (n) of the space-time. Li et al. [10] proved that the Kerr-AdS black hole space-time could be act as a particle accelerator. Studies were done by Zhong et al.[11] for RN-de-Sitter black hole and found that infinite energy in the CM frame near the cosmological horizon. Said et al. [12] studied the particle accelerations and collisions in the back ground of a cylindrical black holes. In [13], the authors suggested that using collisional Penrose process the emitted massive particles can only be gain ~ 30 percentage of the initial rest energy of the in-falling particles.

In [14], the authors discussed the CM energy for the Kerr-Newman black hole. For Kerr-Sen black hole, the CM energy is diverging also discussed in [15]. It was discussed in [16] regarding the BSW process for spherically symmetric RN black hole. Zhu et al. [17] showed that general stationary charged black holes as charge particle accelerators. In [19], the author demonstrated that a weakly magnetized black hole may behave as a particle accelerators. The BSW process was considered for regular black hole, BTZ black hole and Einstein-Maxwell-Dilation-Axion in [18]. The effect of particle accelerations and collisions on the near horizon surface of some black holes was discussed in [20].

Also McWilliams [21] showed that the black holes are neither particle accelerators nor dark matter probes. Galajinsky [22] also showed that the CM energy in the context of the near horizon geometry of the extremal Kerr black holes and proved that the CM energy is finite for any value of the particle parameters. Tursunov et al. [23] studied the particle accelerations and collisions in case of black string. Fernando [24] has studied the possibility of high CM energy of two particles colliding near the infinite red-shift surface of a charged black hole in string theory. Studies of BSW effect were performed in [25, 26] for the naked singularity case of different space-times.

In a recent work [27], we have demonstrated that an extremal static, spherically symmetric string black hole could act as a particle accelerator with arbitrarily high energy when two uncharged particles falling freely from rest to infinity on the near horizon. It was also shown there that, the CM energy of collision is independent of the extreme fine tuning of the angular momentum parameter of the colliding particles.

In a present work, our objective is to show an analogous effect of particle collisions with a high CM energy is also possible when the black hole is precisely *extremal regular* static and spherically symmetric black hole.

Traditional black holes like Schwarzschild black hole, RN black hole, Kerr black hole and Kerr-Newman black holes have possessed a curvature singularity. Whereas the regular black hole does not possess any curvature singularity. This is the main difference between the traditional black hole and the regular black hole. On the other hand, it is also important to understand the final state of gravitational collapse of initially regular

configurations we need to study the global regularity of black hole solutions. Broadly speaking, for traditional black holes the curvature invariants $R, R_{ab}R^{ab}, R_{abcd}R^{abcd}$ blows up at $r = 0$ in the spacetime manifold, while for regular black holes the curvature invariants do not blow up everywhere in the spacetime manifold including at $r = 0$. In this sense it is said "regular black hole" or "non-singular black hole".

We have considered here a number of regular black holes like: the Bardeen black hole [28], Ayón-Beato & García (ABG) black hole [29] and Hayward black hole [30]. The special features of these black holes are they have satisfied the weak energy condition(WEC) and the energy-momentum tensor should have the symmetry $T_{00} = T_{11}$. Our goal here is to see what happens the BSW effect for these black holes in the *extremal limit*.

Circular geodesic motion in the equatorial plane is of fundamental interest in black hole physics as well as in accretion disk physics to determine the important features of the spacetime. Circular orbits with $r > r_{ISCO}$ are stable, while those with $r < r_{ISCO}$ are not. Keplerian circular orbits exist in the region $r > r_{ph}$, with r_{ph} being the circular photon orbit. Bound circular orbits exist in the region $r > r_{mb}$, with r_{mb} being the marginally bound circular orbit, and stable circular orbits exist for $r > r_{ISCO}$, with r_{ISCO}. We have calculated these orbits for the above regular black holes. These orbits are very crucial in black hole physics as well as in astrophysics because they determine important information on the back ground geometry.

There are a number of references we would like to mention here which discuss the some interesting properties of the regular black holes. Firstly, Ansoldi [33] gives a good review about the regular black hole. Balart [34] studied the Brown-York quasi-local energy and Komar energy at the horizon which is called Bose-Dadhich identity [35], and proved that this identity does not satisfy for regular black holes. In [36], the author showed that Smarr's formula do not satisfy in case of the regular Bardeen and ABG space-time. In [37], the authors have studied the weak energy condition of the regular black hole. Recently, García et al. [38] have discussed the complete geodesic structure of ABG spacetime by using Weierstrass elliptic functions. Finally, Eiroa et al. [39] have discussed the gravitational lensing effect of the regular Bardeen black hole.

The paper is organized as follows. In section 2, we compute the CM energy of the particle collision near the infinite red-shift surface of the Bardeen Space-time. In section 3, we describe the BSW effect of the ABG space-time. In section 4, we calculate the E_{cm} for the Hayward black hole and finally we summarize the results in section 5.

2 CM energy of the collision near the horizon of the Bardeen Space-time:

In this section, we shall first examine the CM energy of collision for two neutral particles falling freely from rest at infinity in the horizon of a Bardeen black hole- the *first* regular (singularity-free) black hole model in general relativity(GR). The space-time has an inter-

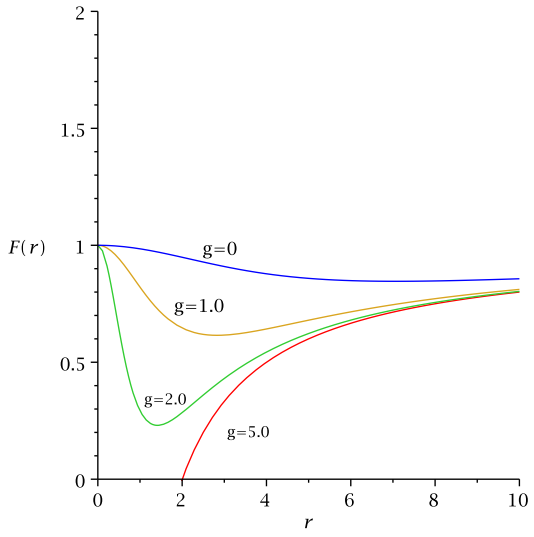

Figure 1: The figure shows the variation of $\mathcal{F}(r)$ with r for different values of g. Here, $m = 1$, $g = 0$ is the Schwarzschild case.

esting feature: it is interpreted as the gravitational field of a nonlinear monopole, i.e., as a magnetic solution to Einstein field equations coupled to a non-linear electrodynamics. To compute the CM energy near the horizon of the regular Bardeen black hole, we first need to know the geodesic structure of this black hole and four velocity of the particles.

2.1 Equatorial circular orbit in the Bardeen space-time:

Thus the line element for the Bardeen space-time[28, 31, 32, 33, 40] is given by

$$ds^2 = -\mathcal{F}(r)dt^2 + \frac{dr^2}{\mathcal{F}(r)} + r^2\left(d\theta^2 + \sin^2\theta d\phi^2\right) \ . \tag{1}$$

where the function $\mathcal{F}(r)$ is defined by

$$\mathcal{F}(r) \ = \ 1 - \frac{2mr^2}{(r^2+g^2)^{\frac{3}{2}}}. \tag{2}$$

where m is the mass of the black hole and g is the monopole charge of the non-linear self gravitating magnetic field. We can see the behaviour of the function $\mathcal{F}(r)$ for different values of g in the following plot.

It may be noted that this metric function behaves asymptotically i.e at $r \to \infty$ as [32]

$$\mathcal{F}(r) \sim 1 - \frac{2m}{r} + \frac{3mg^2}{r^3} + O(\frac{1}{r^5}) \ . \tag{3}$$

Furthermore, if $r \to 0$, the metric function behaves as the de-Sitter space-time, that is

$$\mathcal{F}(r) \sim 1 - \frac{2m}{g^3} r^2 \ . \tag{4}$$

The Bardeen black hole has an event horizon (r_+) which occur at $F(r_+) = 0$. i.e.

$$r_+^6 + (3g^2 - 4m^2) r_+^4 + 3g^4 r_+^2 + g^6 \ = \ 0 \ . \tag{5}$$

The largest real positive root of the equation gives the event horizon (r_+) of the Bardeen black hole is given by

$$r_+ \ = \ \frac{m}{\sqrt{3}} \frac{\sqrt{\left[16 - 24\left(\frac{g}{m}\right)^2 + \{4 - 3\left(\frac{g}{m}\right)^2\} x^{\frac{1}{3}} + x^{\frac{2}{3}}\right]}}{x^{\frac{1}{6}}} \ . \tag{6}$$

where,

$$x = 64 - 144\left(\frac{g}{m}\right)^2 + 54\left(\frac{g}{m}\right)^4 + 6\sqrt{3}\left(\frac{g}{m}\right)^3 \sqrt{27\left(\frac{g}{m}\right)^2 - 16} \ . \tag{7}$$

In the limit $g \to 0$, we recover the horizon of the Schwarzschild black hole i.e. $r_+ = 2m$.

The Bardeen space-time represents a regular black hole when $27g^2 \leq 16m^2$. When $27g^2 < 16m^2$, there are two horizons in the Bardeen space-time, we may call it non-extremal Bardeen space-time as in the non-extremal RN space-time. When $27g^2 = 16m^2$, the two horizons are coincident, which correspond to an extreme Bardeen black hole as in the RN black hole.

To derive the complete geodesic structure of the Bardeen black hole we shall follow the pioneer book of S. Chandrasekhar [41] and J. B. Hartle [42]. To compute the geodesic motion of the test particle in the equatorial plane we set $\dot{\theta} = 0$ and $\theta = constant = \frac{\pi}{2}$. Since the space-time admits two Killing vectors namely, $\zeta \equiv \partial_t$ and $\chi \equiv \partial_\phi$. Therefore the quantities $E = -\zeta \cdot \mathbf{u}$ and $L \equiv \chi \cdot \mathbf{u}$ are conserved along the geodesics, $\mathbf{u}$ is the four velocity of the particle. Where E and L can be interpreted as conserved energy and conserved angular momentum per unit mass respectively.

Thus in this coordinate chart, E can be written as

$$E \ = \ -\zeta \cdot \mathbf{u} = \mathcal{F}(r)\, u^t \ . \tag{8}$$

and, L can be expressed as in terms of the metric

$$r^2\, u^\phi = L \ . \tag{9}$$

From the normalization condition of the four velocity for massive particles we find

$$\mathbf{u}^2 \;=\; \sigma \; . \tag{10}$$

where $\sigma = -1$ for time-like geodesics, $\sigma = 0$ for light-like geodesics and $\sigma = +1$ for space-like geodesics.

Solving (8) and (9) for u^t and u^ϕ we get

$$u^t \;=\; \frac{E}{\mathcal{F}(r)} \; . \tag{11}$$

$$u^\phi \;=\; \frac{L}{r^2} \; . \tag{12}$$

where E and L are the energy and angular momentum per unit mass of the test particle. Substituting these equations in (11) and (12) in (10), we obtain the radial equation for the Bardeen space-time:

$$(u^r)^2 = E^2 - \mathcal{V}_{eff} = E^2 - \left(\frac{L^2}{r^2} - \sigma\right)\mathcal{F}(r) \; . \tag{13}$$

where the standard effective potential for the geodesic motion of the Bardeen space-time is given by

$$\mathcal{V}_{eff} = \left(\frac{L^2}{r^2} - \sigma\right)\left(1 - \frac{2mr^2}{(r^2+g^2)^{\frac{3}{2}}}\right) \; . \tag{14}$$

2.1.1 Particle orbits:

The effective potential for time-like geodesics can be obtained from the above equation (13) by putting $\sigma = -1$ as

$$\mathcal{V}_{eff} \;=\; \left(1 + \frac{L^2}{r^2}\right)\left(1 - \frac{2mr^2}{(r^2+g^2)^{\frac{3}{2}}}\right) \; . \tag{15}$$

To derive the circular geodesic motion of the test particle in Bardeen space-time, we must impose the condition $\dot{r} = 0$ at $r = r_0$. Thus one gets from equation (13)

$$\mathcal{V}_{eff} \;=\; E^2 \; . \tag{16}$$

and,

$$\frac{d\mathcal{V}_{eff}}{dr} \;=\; 0 \; . \tag{17}$$

Thus one can obtain the energy and angular momentum per unit mass of the test particle along the circular orbits are:

$$E_0^2 = \frac{\left[(r_0^2+g^2)^{\frac{3}{2}}-2mr_0^2\right]^2}{\sqrt{r_0^2+g^2}\left[(r_0^2+g^2)^{\frac{5}{2}}-3mr_0^4\right]} . \tag{18}$$

and,

$$L_0^2 = \frac{mr_0^4\,(r_0^2-2g^2)}{\left[(r_0^2+g^2)^{\frac{5}{2}}-3mr_0^4\right]} . \tag{19}$$

Circular motion of the test particle to be exists when both energy and angular momentum are real and finite.

Thus we must have

$$(r_0^2+g^2)^{\frac{5}{2}}-3mr_0^4>0 \text{ and } r_0>\sqrt{2}g . \tag{20}$$

Circular orbits do not exist for all values of r, so from Eq. (18) and Eq. (19), we can see that the denominator would be real only when

$$(r_0^2+g^2)^{\frac{5}{2}}-3mr_0^4\geq 0 .$$

or

$$r_0^{10}+(5g^2-9m^2)r_0^8+10g^4r_0^6+10g^6r_0^4+5g^8r_0^2+g^{10}\geq 0$$

The limiting case of equality gives a circular orbit with infinite energy per unit rest mass i.e. a photon orbit. This photon orbit is the inner most boundary of the circular orbit for massive particles.

One can obtain MBCO for Bardeen space-time can be written as :

$$r_0^6+(9g^2-16m^2)r_0^4+24g^4r_0^2+16g^6=0 . \tag{21}$$

Let $r_0=r_{mb}$ be the solution of the equation which gives the radius of MBCO.

From astrophysical point of view the most important class of orbits are ISCOs which can be derived from the second derivative of the effective potential of time-like case. i.e.

$$\frac{d^2\mathcal{V}_{eff}}{dr^2} = 0 \tag{22}$$

Thus one may get the ISCO equation for the Bardeen space-time reads as

$$r_0^{14}+(19g^2-36m^2)r_0^{12}+99g^4r_0^{10}+65g^6r_0^8-$$

$$160g^8r_0^6-144g^{10}r_0^4+64g^{12}r_0^2+64g^{14} = 0 . \tag{23}$$

Let $r_0=r_{ISCO}$ be the real solution of the equation (23) which gives the radius of the ISCO of Bardeen space-time.

In the limit $g\to 0$, we obtain the radius of ISCO for Schwarzschild black hole which is $r_{ISCO}=6m$.

2.1.2 Photon orbits:

For null circular geodesics, the effective potential becomes

$$\mathcal{U}_{eff} = \frac{L^2}{r^2}\mathcal{F}(r) = \frac{L^2}{r^2}\left(1 - \frac{2mr^2}{(r^2+g^2)^{\frac{3}{2}}}\right) \tag{24}$$

For circular null geodesics at $r = r_c$, we find

$$\mathcal{U}_{eff} = E^2 \tag{25}$$

and,

$$\frac{d\mathcal{U}_{eff}}{dr} = 0 \tag{26}$$

Thus one may obtain the ratio of energy and angular momentum of the test particle evaluated at $r = r_c$ for circular photon orbits are:

$$\frac{E_c}{L_c} = \pm\sqrt{\frac{(r_c^2+g^2)^{\frac{3}{2}} - 2mr_c^2}{r_c^2(r_c^2+g^2)^{\frac{3}{2}}}} \tag{27}$$

and,

$$r_c^{10} + (5g^2 - 9m^2)r_c^8 + 10g^4 r_c^6 +$$

$$10g^6 r_c^4 + 5g^8 r_c^2 + g^{10} = 0. \tag{28}$$

Let $r_c = r_{ph}$ be the solution of the equation (28) which gives the radius of the CPO of the Bardeen space-time. In the limit $g \to 0$, we obtain the radius of photon orbit for Schwarzschild black hole which is $r_{ph} = 3m$.

Let $D_c = \frac{L_c}{E_c}$ be the impact parameter for null circular geodesics then

$$\frac{1}{D_c} = \frac{E_c}{L_c} = \sqrt{\frac{(r_c^2+g^2)^{\frac{3}{2}} - 2mr_c^2}{r_c^2(r_c^2+g^2)^{\frac{3}{2}}}} \tag{29}$$

In the limit $g \to 0$, we obtain the impact parameter of the CPO for the Schwarzschild black hole which is $D_c = 3\sqrt{3}m$.

2.2 CM energy and Particle collision:

Now let us compute the CM energy for the collision of two neutral particles of same rest mass m_0 but different energy coming from infinity with $\frac{E_1}{m_0} = \frac{E_2}{m_0} = 1$ and approaching the event horizon (infinite red-shift surface) of the Bardeen black hole with different angular

momenta L_1 and L_2. Since our background is curved, so we need to define the CM frame properly. BSW [1] have been first derived the simple formula which is valid in both flat and curved spacetime:

$$\left(\frac{E_{cm}}{\sqrt{2}m_0}\right)^2 = 1 - g_{\mu\nu}u^{\mu}_{(1)}u^{\nu}_{(2)} \ . \tag{30}$$

where $u^{\mu}_{(1)}$ and $u^{\mu}_{(2)}$ are the four velocity of the particles, properly normalized by $\mathbf{u}.\mathbf{u} = -1$ (we have used the signature in the meric is (-+++)). This formula is of course well known in special relativity and in general relativity to ensure its validity.

We also assume throughout this work the geodesic motion of the colliding particles confined in the equatorial plane. As we have previously said that the Bardeen spacetime admits a time-like isometry followed by the time-like Killing vector field ζ whose projection along the four velocity $\mathbf{u}$ of geodesics $\zeta.\mathbf{u} = -E$, is conserved along such geodesics. Similarly there is also the 'angular momentum' $L = \chi.\mathbf{u}$ is conserved due to the rotational symmetry(where $\chi \equiv \partial_\phi$). For time-like particles, the components of the four velocity are

$$u^t = \dot{t} = \frac{E}{\mathcal{F}(r)} \tag{31}$$

$$u^r = \dot{r} = \pm\sqrt{E^2 - \mathcal{F}(r)\left(1 + \frac{L^2}{r^2}\right)} \tag{32}$$

$$u^\theta = \dot{\theta} = 0 \tag{33}$$

$$u^\phi = \dot{\phi} = \frac{L}{r^2} \ . \tag{34}$$

and,

$$u^{\mu}_{(1)} = \left(\frac{E_1}{\mathcal{F}(r)}, \ -X_1, \ 0, \ \frac{L_1}{r^2}\right) \ . \tag{35}$$

$$u^{\mu}_{(2)} = \left(\frac{E_2}{\mathcal{F}(r)}, \ -X_2, \ 0, \ \frac{L_2}{r^2}\right) \ . \tag{36}$$

where

$$X_1 = \sqrt{E_1^2 - \mathcal{F}(r)\left(1 + \frac{L_1^2}{r^2}\right)} \tag{37}$$

$$X_2 = \sqrt{E_2^2 - \mathcal{F}(r)\left(1 + \frac{L_2^2}{r^2}\right)} \tag{38}$$

Substituting this in (30), we get the CM energy:

$$\left(\frac{E_{cm}}{\sqrt{2}m_0}\right)^2 = 1 + \frac{E_1E_2}{\mathcal{F}(r)} - \frac{X_1X_2}{\mathcal{F}(r)} - \frac{L_1L_2}{r^2} \ . \tag{39}$$

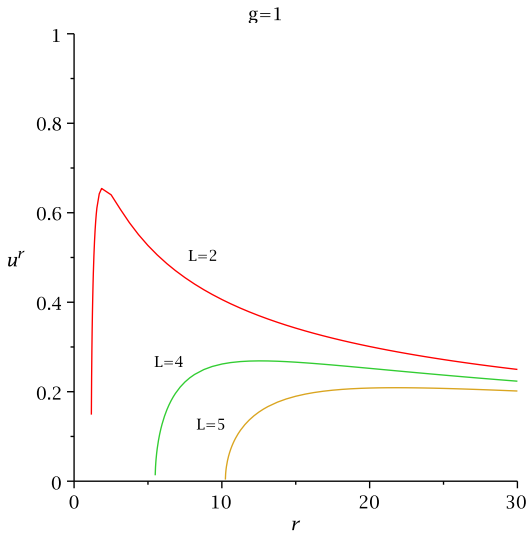

Figure 2: The figure shows the variation of $\dot{r}$ with r for Bardeen black hole. Here, $m = 1$.

The figures[2,3,4] depict the variation of radial velocity with r and the variation of CM energy with r for Bardeen black hole.

For simplicity, $E_1 = E_2 = 1$ and substituting the value of $\mathcal{F}(r)$, we obtain the CM energy near the event horizon (r_+) of the Bardeen space-time:

$$E_{cm}\mid_{r\to r_+} = \sqrt{2}m_0\sqrt{\frac{4r_+^2+(L_1-L_2)^2}{2r_+^2}}\ . \tag{40}$$

where r_+ is described in equation (6).

When we set $r_+ = 2m$, we recover the CM energy of the Schwarzschild black hole [[1]]:

$$E_{cm} = \sqrt{2}m_0\sqrt{\frac{16m^2+(L_1-L_2)^2}{8m^2}}\ . \tag{41}$$

It is known that the maximum CM energy of the Schwarzschild black hole occurs for the critical values of angular momentum parameter i.e. $L_1 = 4m$ and $L_2 = -4m$. Its value near the horizon is $2\sqrt{5}m_0$ [43].

The angular velocity of the Bardeen space-time at the r_+ is given by

$$\Omega_H = \frac{\dot{\phi}}{\dot{t}} = \sqrt{\frac{m(r_0^2-2g^2)}{(r_0^2+g^2)^{\frac{5}{2}}}}\ . \tag{42}$$

The critical angular momenta L_i can be written as

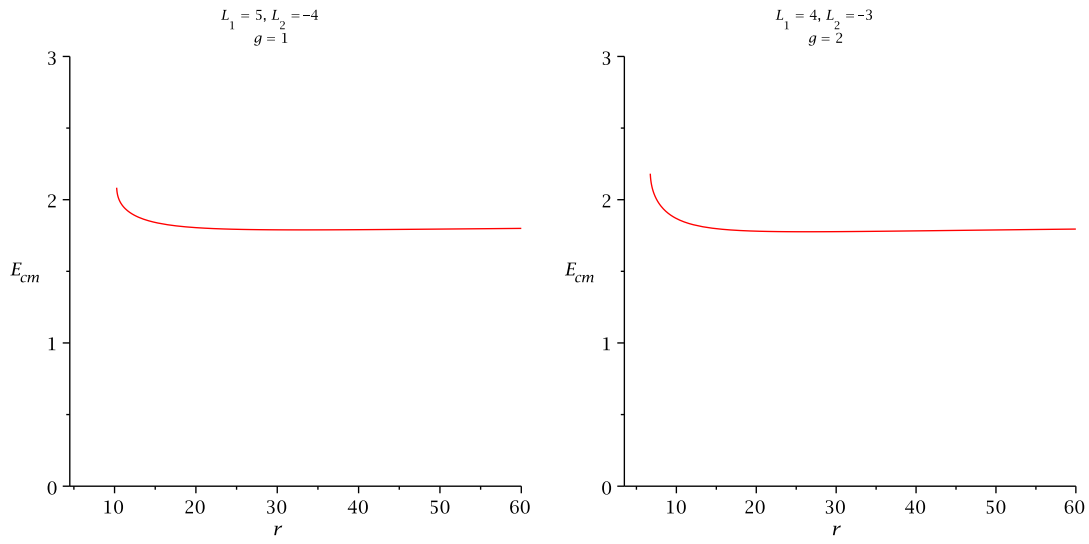

Figure 3: The figure shows the variation of E_{cm} with r for Bardeen black hole.

$$L_i \;=\; \frac{E_i}{\Omega_H}\,. \tag{43}$$

In the extremal cases, when $27g^2 = 16m^2$, the horizon is at $r_0 = 1.08m$ and it has been already mentioned in [1], a new phenomenon would appear if one of the particles participating in the collision has the critical angular momentum. If one of the particles have the diverging angular momentum at the horizon i.e.

$$L_1 \mid_{r_0=1.08M} \rightarrow \infty\,. \tag{44}$$

Then for extremal Bardeen space-time, we get the infinite amounts of CM energy, i.e.

$$E_{cm} \;\longmapsto\; \infty\,. \tag{45}$$

3 CM energy of the collision near the horizon of the Ayón-Beato and García Space-time:

In this section, we will investigate the CM energy of collision for two neutral particles falling freely from rest at infinity in the horizon of a ABG black hole. This space-time is also a regular black hole space-time and singularity free solutions of the coupled system of a non-linear electrodynamics and general relativity. The source is a nonlinear electrodynamic field satisfying the WEC, which in the limit of weak field becomes the Maxwell

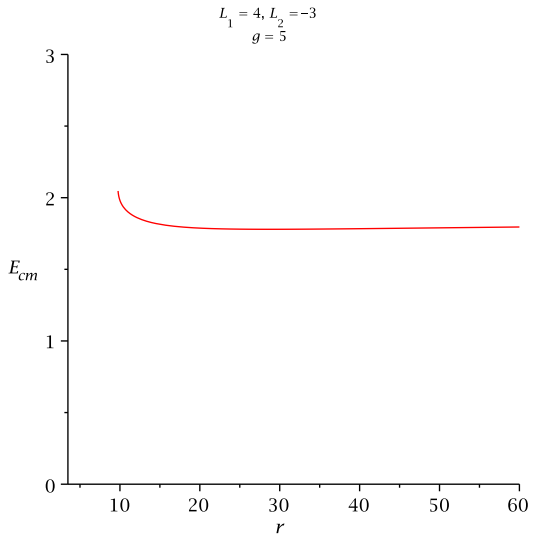

Figure 4: The figure shows the variation of E_{cm} with r for Bardeen black hole with different values of angular momentum. Here $g = 5$.

field. We find the CM energy for this space-time can be infinitely high when the black hole is only *extremal*. Before computing the CM energy we shall demonstrate shortly the geodesic structure of the ABG space-time.

3.1 Equatorial circular orbit in the ABG space-time:

The metric of the ABG space-time [29, 44, 45, 46, 38] is given by

$$ds^2 = -\mathcal{G}(r)dt^2 + \frac{dr^2}{\mathcal{G}(r)} + r^2\left(d\theta^2 + \sin^2\theta d\phi^2\right) \ . \tag{46}$$

where the function $\mathcal{G}(r)$ is defined by

$$\mathcal{G}(r) \ = \ 1 - \frac{2mr^2}{(r^2+q^2)^{\frac{3}{2}}} + \frac{q^2r^2}{(r^2+q^2)^2} \ . \tag{47}$$

where m is the mass of the black hole and q is the monopole charge. The strength of the radial electric field E_r is given by

$$E_r \ = \ qr^4\left(\frac{r^2-5q^2}{(r^2+q^2)^4} + \frac{15}{2}\frac{m}{(r^2+q^2)^{7/2}}\right) \ . \tag{48}$$

We can see the behaviour of the function $\mathcal{G}(r)$ graphically.

This is also a first regular black hole solution in general relativity. The source is a nonlinear electrodynamic field satisfying the WEC, which in the limit of weak field becomes the Maxwell field.

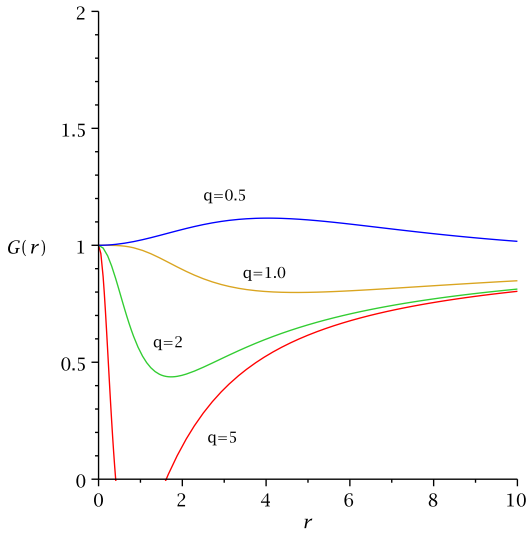

Figure 5: The figure shows the variation of $\mathcal{G}(r)$ with r for different values of q. Here, $m = 1$.

It may also be noted that this metric function asymptotically behaves as the RN space-time[29] i.e.,

$$\mathcal{G}(r) \sim 1 - \frac{2m}{r} + \frac{q^2}{r^2} + O(\frac{1}{r^3}),$$
$$E_r \sim \frac{q}{r^2} + O(\frac{1}{r^3}) \ . \tag{49}$$

The ABG black hole has an event horizon (r_+) which occur at $G(r_+) = 0$. i.e.

$$r_+^8 + (6q^2 - 4m^2)r_+^6 + (11q^4 - 4m^2q^2)r_+^4$$
$$+6q^6 r_+^2 + q^8 = 0 \ . \tag{50}$$

In the limit $q \to 0$, we shall get the horizon of the Schwarzschild black hole i.e. $r_+ = 2m$. The ABG space-time represents a regular black hole when $\mid q \mid \leq q_c$. The value of q_c is $q_c \approx 0.634m$. When $\mid q \mid \leq q_c$, there are two horizons in the ABG space-time, we call it non-extremal ABG space-time as in the non-extremal RN space-time.

When $\mid q \mid = q_c$, the two horizons are coincident at $r_+ \sim 1.005m$, which corresponds to an extreme ABG black hole as in the RN black hole. The Carter-Penrose diagram of ABG space-time is quite similar structure to the RN black hole.

Proceeding analogously as in section 2, the radial equation that governs the geodesic structure in the ABG space-time reads

$$(u^r)^2 = \dot{r}^2 = E^2 - \mathcal{V}_{eff} = E^2 - \left(\frac{L^2}{r^2} - \sigma\right)\mathcal{G}(r) \ . \tag{51}$$

where the effective potential for the geodesic motion of the ABG space-time is given by

$$\mathcal{V}_{eff} = \left(\frac{L^2}{r^2} - \sigma\right)\left(1 - \frac{2mr^2}{(r^2+q^2)^{\frac{3}{2}}} + \frac{q^2r^2}{(r^2+q^2)^2}\right) \ . \tag{52}$$

3.1.1 Particle orbits:

The effective potential for time-like geodesics can be written as using the equation (51) by setting $\sigma = -1$:

$$\mathcal{V}_{eff} = \left(1 + \frac{L^2}{r^2}\right)\left(1 - \frac{2mr^2}{(r^2+q^2)^{\frac{3}{2}}} + \frac{q^2r^2}{(r^2+q^2)^2}\right) \ . \tag{53}$$

To derive the circular geodesic motion of the test particle in ABG space-time, we must use the condition $\dot{r} = 0$ at $r = r_0$. From equation (51), one gets

$$\mathcal{V}_{eff} \ = \ E^2 \ . \tag{54}$$

and

$$\frac{d\mathcal{V}_{eff}}{dr} \ = \ 0 \ . \tag{55}$$

Thus one can obtain the energy and angular momentum per unit mass of the test particle along the circular orbits :

$$E_0^2 = \frac{\left[(r_0^2+q^2)^2 - 2mr_0^2\sqrt{r_0^2+q^2} + q^2r_0^2\right]^2}{(r_0^2+q^2)\left[(r_0^2+q^2)^3 - 3mr_0^4\sqrt{r_0^2+q^2} + 2q^2r_0^4\right]} \ . \tag{56}$$

and,

$$L_0^2 = \frac{r_0^4\left[m(r_0^2-2q^2)\sqrt{r_0^2+q^2} - q^2(r_0^2-q^2)\right]}{\left[(r_0^2+q^2)^3 - 3mr_0^4\sqrt{r_0^2+q^2} + 2q^2r_0^4\right]} \ . \tag{57}$$

Circular motion of the test particle to be exists for ABG space-time when both energy and angular momentum are real and finite.

Thus we get the inequality:

$$(r_0^2+q^2)^3 - 3mr_0^4\sqrt{r_0^2+q^2} + 2q^2r_0^4 > 0$$

and

$$r_0 > q\sqrt{\frac{2m\sqrt{r_0^2+q^2}-q^2}{m\sqrt{r_0^2+q^2}-q^2}}\ .$$

Circular orbits do not exist for all values of r, so from Eq. (56) and Eq. (57), we can see that the denominator would be real only when

$$(r_0^2+q^2)^3 - 3mr_0^4\sqrt{r_0^2+q^2} + 2q^2r_0^4 \ \geq\ 0\ . \tag{58}$$

or

$$r_0^{12} + (10q^2-9m^2)r_0^{10} - (9m^2q^2-31q^4)r_0^8 +$$
$$32q^6r_0^6 + 19q^8r_0^4 + 6q^{10}r_0^2 + q^{12} \ \geq\ 0 \tag{59}$$

The limiting case of equality indicates a circular orbit with diverging energy per unit rest mass i.e. a photon orbit. This photon orbit is the inner most boundary of the circular orbits for time-like particles.

The equation of MBCO for ABG space-time looks like:

$$m^2r_0^{10} - (16m^4-3m^2q^2)r_0^8 +$$
$$(99m^2q^4-32m^4q^2)r_0^6 - (16m^4q^4-23m^2q^6-9q^8)r_0^4 +$$
$$(72m^2q^8-12q^{10})r_0^2 + (16m^2q^{10}-4q^{12}) \ =\ 0\ . \tag{60}$$

Let $r_0 = r_{mb}$ be the solution of the equation which gives the radius of MBCO close to the black hole.

The ISCO equation can be obtained from the second derivative of the effective potential of time-like case. i.e.

$$\frac{d^2\mathcal{V}_{eff}}{dr^2} \ =\ 0 \tag{61}$$

Thus one may get the ISCO equation for the ABG space-time reads as

$$m^2r_0^{18} - (36m^4-39m^2q^2+4q^4)r_0^{16} +$$
$$(97m^2q^4-72m^4q^2+40q^6)r_0^{14} - (36m^4q^4-97m^2q^6+52q^8)r_0^{12}$$
$$-(89m^2q^8+216q^{10})r_0^{10} - (357m^2q^{10}+272q^{12})r_0^8 -$$
$$(292m^2q^{12}+104q^{14})r_0^6 + (16m^2q^{14}+12q^{16})r_0^4 +$$
$$(144m^2q^{16}+24q^{18})r_0^2 + 4q^{18}(16m^2-q^2) \ =\ 0\ . \tag{62}$$

Let $r_0 = r_{ISCO}$ be the real solution of the equation (62) which gives the radius of the ISCO of ABG space-time.

In the limit $q \to 0$, we obtain the radius of ISCO for Schwarzschild black hole which is $r_{ISCO} = 6m$.

3.1.2 Photon orbits:

For null circular geodesics, the effective potential becomes

$$\begin{aligned}\mathcal{U}_{eff} &= \frac{L^2}{r^2}\mathcal{G}(r) \\ &= \frac{L^2}{r^2}\left(1-\frac{2mr^2}{(r^2+q^2)^{\frac{3}{2}}}+\frac{q^2r^2}{(r^2+q^2)^2}\right) \end{aligned} \tag{63}$$

For circular null geodesics at $r = r_c$, we find

$$\mathcal{U}_{eff} = E^2 \tag{64}$$

and,

$$\frac{d\mathcal{U}_{eff}}{dr} = 0 \tag{65}$$

Thus one may obtain the ratio of energy and angular momentum of the test particle evaluated at $r = r_c$ for CPO is

$$\frac{E_c}{L_c} = \pm\sqrt{\frac{1}{r_c^2}\left(1-\frac{2mr_c^2}{(r_c^2+q^2)^{\frac{3}{2}}}+\frac{q^2r_c^2}{(r_c^2+q^2)^2}\right)} \tag{66}$$

and,

$$\begin{aligned} r_c^{12}+(10q^2-9m^2)r_c^{10}-(9m^2q^2-31q^4)r_c^8+ \\ 32q^6r_c^6+19q^8r_c^4+6q^{10}r_c^2+q^{12} = 0. \end{aligned} \tag{67}$$

Let $D_c = \frac{L_c}{E_c}$ be the impact parameter for null circular geodesics then

$$\frac{1}{D_c} = \frac{E_c}{L_c} = \sqrt{\frac{1}{r_c^2}\left(1-\frac{2mr_c^2}{(r_c^2+q^2)^{\frac{3}{2}}}+\frac{q^2r_c^2}{(r_c^2+q^2)^2}\right)} \tag{68}$$

Let $r_c = r_{ph}$ be the solution of the equation (67) which gives the radius of the photon orbit of the ABG space-time. In the limit $q \to 0$, we recover the CPO of Schwarzschild black hole which is $r_{ph} = 3m$.

3.2 CM Energy for ABG space-time:

Now let us compute the CM energy for the collision of two neutral particles coming from infinity with $\frac{E_1}{m_0} = \frac{E_2}{m_0} = 1$ and approaching the ABG space-time with different angular momenta L_1 and L_2.

Since the ABG space-time has also Killing symmetries followed by the Killing vector field thus energy (E) and angular momentum (L) are conserved quantities as we have defined in case of Bardeen space-time.

Therefore for massive particles of ABG space-time, the components of the four velocity are

$$u^t = \frac{E}{\mathcal{G}(r)} \tag{69}$$

$$u^r = \pm\sqrt{E^2 - \mathcal{G}(r)\left(1 + \frac{L^2}{r^2}\right)} \tag{70}$$

$$u^\theta = 0 \tag{71}$$

$$u^\phi = \frac{L}{r^2}\,. \tag{72}$$

and,

$$u^\mu_{(1)} = \left(\frac{E_1}{\mathcal{G}(r)},\ -Y_1,\ 0,\ \frac{L_1}{r^2}\right)\,. \tag{73}$$

$$u^\mu_{(2)} = \left(\frac{E_2}{\mathcal{G}(r)},\ -Y_2,\ 0,\ \frac{L_2}{r^2}\right)\,. \tag{74}$$

where

$$Y_1 = \sqrt{E_1^2 - \mathcal{G}(r)\left(1 + \frac{L_1^2}{r^2}\right)} \tag{75}$$

$$Y_2 = \sqrt{E_2^2 - \mathcal{G}(r)\left(1 + \frac{L_2^2}{r^2}\right)} \tag{76}$$

We can see graphically the variation of $\dot{r}$ with r and the variation of CM energy with r for ABG space-time.

Substituting this in (30), we get the center of mass energy for ABG space-time:

$$\left(\frac{E_{cm}}{\sqrt{2}m_0}\right)^2 = 1 + \frac{E_1E_2}{\mathcal{G}(r)} - \frac{Y_1Y_2}{\mathcal{G}(r)} - \frac{L_1L_2}{r^2}\,. \tag{77}$$

For simplicity, $E_1 = E_2 = 1$ and putting the value of $\mathcal{G}(r)$, we obtain the CM energy near the event horizon (r_+) of the ABG space-time:

$$E_{cm}\,|_{r\to r_+} = \sqrt{2}m_0\sqrt{\frac{4r_+^2 + (L_1 - L_2)^2}{2r_+^2}}\,. \tag{78}$$

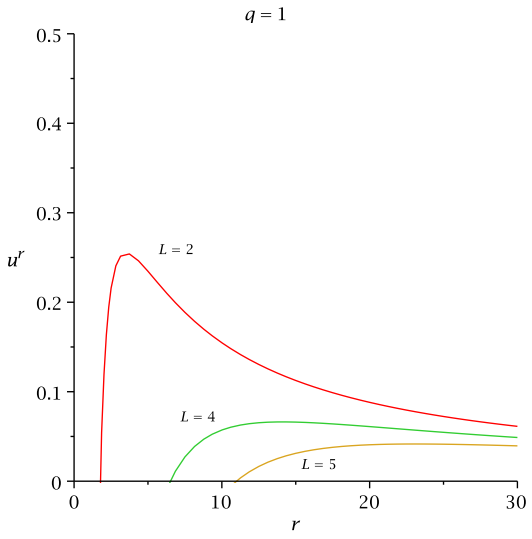

Figure 6: The figure shows the variation of $\dot{r}$ with r for ABG space-time. Here, $m = 1, q = 1$.

where r_+ is the root of the given Eq. in (50) .

When we set $r_+ = 2m$, we get the CM energy of the Schwarzschild black hole:

$$E_{cm} \quad = \quad \sqrt{2}m_0\sqrt{\frac{16m^2 + (L_1 - L_2)^2}{8m^2}} \ . \tag{79}$$

The angular velocity of the ABG space-time at the event horizon r_+ is given by

$$\Omega_H = \frac{\dot{\phi}}{\dot{t}} = \sqrt{\frac{m(r_0^2 - 2q^2)}{(r_0^2 + q^2)^{\frac{5}{2}}} - \frac{q^2(r_0^2 - q^2)}{(r_0^2 + q^2)^3}} \ . \tag{80}$$

The critical angular momenta L_i may be written as

$$L_i \quad = \quad \frac{E_i}{\Omega_H} \ . \tag{81}$$

At the extremal cases, when $q = q_c$, the horizon is at $r_0 = 1.005m$ and if one of the values of critical angular momenta diverge i.e.

$$L_1 \mid_{r_0 = 1.005M} \rightarrow \infty \ . \tag{82}$$

Therefore for extremal ABG space-time, we obtain the infinite amount of CM energy, i.e.

$$E_{cm} \quad \longmapsto \quad \infty \ . \tag{83}$$

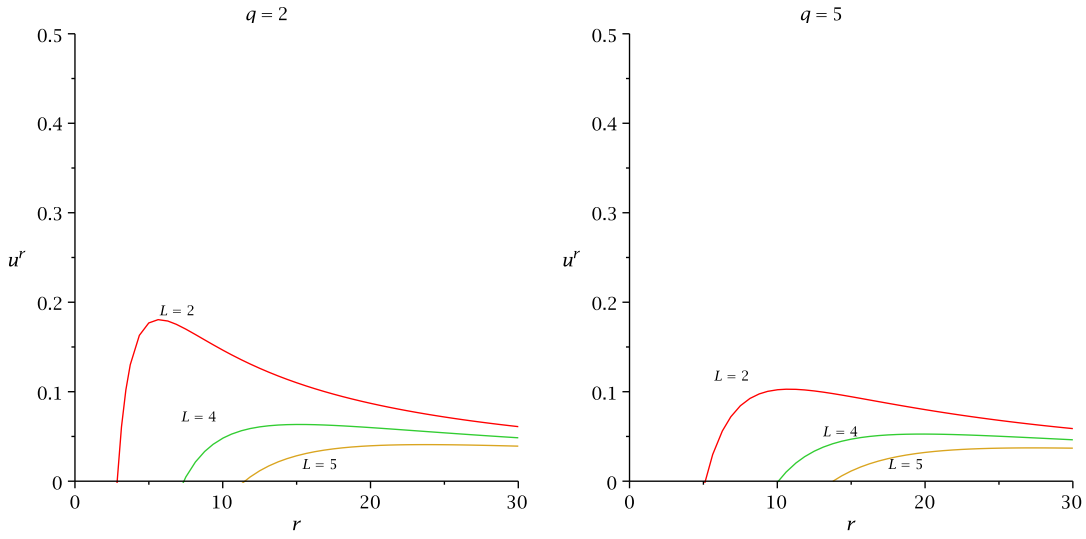

Figure 7: The figure shows the variation of $\dot{r}$ with r for ABG space-time. Here, $m = 1$.

4 CM energy of the collision near the horizon of the Hayward Black hole:

Finally, in this section, we shall perform similar analysis for another interesting regular black hole i.e. Hayward black hole which was suggested by Hayward in 2006 for the process of a regular black hole formation and evaporation.

The line element for the Hayward black hole [30] is given by

$$ds^2 = -\mathcal{H}(r)dt^2 + \frac{dr^2}{\mathcal{H}(r)} + r^2\left(d\theta^2 + \sin^2\theta d\phi^2\right) \ . \tag{84}$$

where the function $\mathcal{H}(r)$ is defined by

$$\mathcal{H}(r) = 1 - \frac{2mr^2}{(r^3 + 2\alpha^2)}. \tag{85}$$

and

$$\alpha^2 = ml^2. \tag{86}$$

where m is the mass of the black hole and l is a free parameter. The behaviour of the metric function $\mathcal{H}(r)$ for Hayward black hole for different values of l can be seen from the following diagram.

Hayward first use such types of metric for the formation and evaporation of a non-singular black hole [30]. The metric describes a static, spherically symmetric and asymptotically flat, have regular centers and for which the resulting energy-momentum tensor

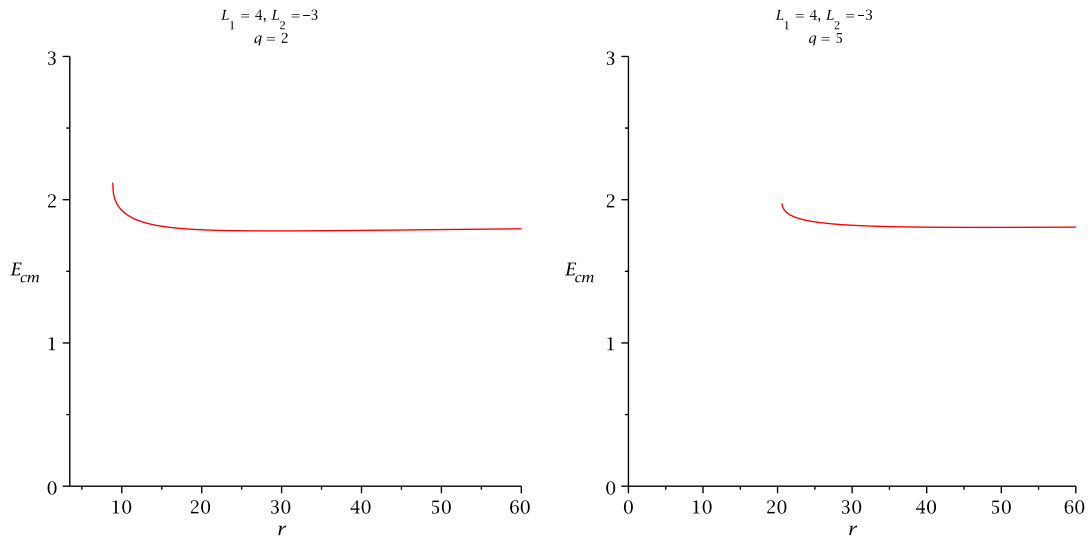

Figure 8: The figure shows the variation of E_{cm} with r for ABG black hole with different values of angular momentum.

satisfying the WEC. The Carter-Penrose diagram is similar to that of RN space-time, with the internal singularities replaced by regular centers.

Noticed that this metric function asymptotically i.e. at $r \to \infty$ behaves as[30]

$$\mathcal{H}(r) \sim 1 - \frac{2m}{r} \ . \tag{87}$$

Furthermore, if $r \to 0$, the metric behaves as the de-Sitter space-time:

$$\mathcal{H}(r) \sim 1 - \frac{r^2}{l^2} \ . \tag{88}$$

The Hayward black hole has an event horizon (r_+) which occur at $H(r_+) = 0$. i.e.

$$r_+^3 - 2mr_+^2 + 2ml^2 \ = \ 0 \ . \tag{89}$$

The largest real positive root of the equation is given by

$$r_+ \ = \ \frac{m}{3}\left[2 + z^{\frac{1}{3}} + \frac{4}{z^{\frac{1}{3}}}\right] \ . \tag{90}$$

where

$$z = 8 - 27\left(\frac{l}{m}\right)^2 + 9\sqrt{3}\left(\frac{l}{m}\right)\sqrt{27\left(\frac{l}{m}\right)^2 - 16} \ . \tag{91}$$

when $l = 0$, we recover the Schwarzschild black hole horizon $(r_+ = 2m)$.

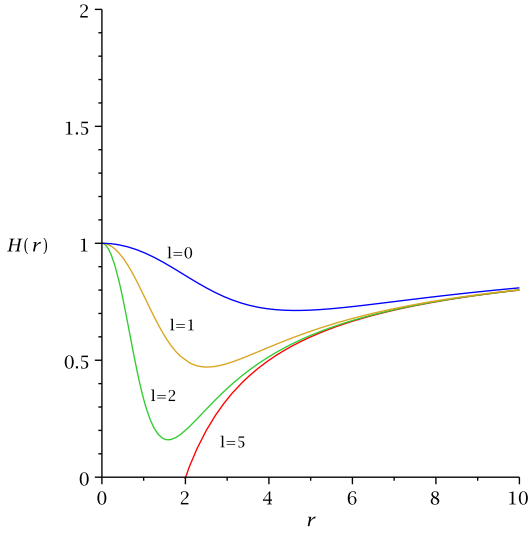

Figure 9: The figure shows the variation of $\mathcal{H}(r)$ with r for different values of l. Here, $m = 1$.

The Hayward space-time represents a regular black hole when $27l^2 \leq 16m^2$.

When $27l^2 < 16m^2$, there are two horizons in the Hayward space-time, we call it non-extremal Hayward space-time.

When $27l^2 = 16m^2$, the two horizons merge, which correspond to an extreme Hayward black hole.

To study the geodesic motion for this space-time we shall perform similar analysis as we have done in section 2 using Killing symmetries.

Thus the radial equation that govern the geodesic motion in the equatorial plane for the Hayward space-time can be written as:

$$(u^r)^2 = E^2 - \mathcal{V}_{eff} = E^2 - \left(\frac{L^2}{r^2} - \sigma\right)\mathcal{H}(r) \ . \tag{92}$$

where the standard effective potential that describe the geodesic motion of the Hayward space-time is

$$\mathcal{V}_{eff} = \left(\frac{L^2}{r^2} - \sigma\right)\left(\frac{2mr^2}{r^3 + 2ml^2}\right) \ . \tag{93}$$

4.0.1 Particle orbits:

The effective potential for time-like geodesics for the Hayward space-time becomes

$$\mathcal{V}_{eff} \ = \ \left(1 + \frac{L^2}{r^2}\right)\left(1 - \frac{2mr^2}{(r^3 + 2l^2m)}\right) \ . \tag{94}$$

To derive the circular geodesic motion of the test particle in the Hayward space-time, we must have the condition $\dot{r} = 0$ at $r = r_0$. Thus one gets, from equation (92)

$$\mathcal{V}_{eff} = E^2 \ . \tag{95}$$

and,

$$\frac{d\mathcal{V}_{eff}}{dr} = 0 \ . \tag{96}$$

A straightforward calculation implies that the energy and angular momentum per unit mass of the test particle along the circular orbits are:

$$E_0^2 = \frac{\left[r_0^3 + 2ml^2 - 2mr_0^2\right]^2}{\left[r_0^6 - 3mr_0^5 + 4ml^2r_0^3 + 4m^2l^4\right]} \ . \tag{97}$$

and,

$$L_0^2 = \frac{mr_0^4\left(r_0^3 - 4ml^2\right)}{\left[r_0^6 - 3mr_0^5 + 4ml^2r_0^3 + 4m^2l^4\right]} \ . \tag{98}$$

The condition for circular motion to be exists in the Hayward space-time when both energy (E_0) and angular momentum (L_0) are real and finite.

Thus we have the condition:

$$r_0^6 - 3mr_0^5 + 4ml^2r_0^3 + 4m^2l^4 > 0 \text{ and } r_0 > (4ml^2)^{\frac{1}{3}} \ . \tag{99}$$

Circular orbits do not exist for all radii, so from Eq. (97) and Eq. (98), we can find that the denominator would be real only when

$$r_0^6 - 3mr_0^5 + 4ml^2r_0^3 + 4m^2l^4 \geq 0 \ . \tag{100}$$

The limiting case of equality gives a circular orbit with infinite energy per unit rest mass i.e. a photon orbit. This photon orbit is the inner most boundary of the circular orbits for massive particles.

One can obtain MBCO for Hayward space-time would be

$$r_0^3 - 4mr_0^2 + 8ml^2 = 0 \ . \tag{101}$$

Using MAPLE software, we can find the real positive root of the Eq.(101) which gives the radius of MBCO closest to the black hole is given by

$$r_{mb} = \frac{m}{3}\left[4 + y^{\frac{1}{3}} + \frac{16}{y^{\frac{1}{3}}}\right] \ . \tag{102}$$

where,

$$y = 64 - 108\left(\frac{l}{m}\right)^2 +$$

$$12\sqrt{3}\left(\frac{l}{m}\right)\sqrt{27\left(\frac{l}{m}\right)^2 - 32}\ . \tag{103}$$

From an astrophysical significance the most important class of orbits are ISCOs which can be calculated from the second derivative of the effective potential of time-like case. i.e.

$$\frac{d^2\mathcal{V}_{eff}}{dr^2} \;=\; 0 \tag{104}$$

Thus one would obtain the ISCO equation for the Hayward space-time:

$$r_0^9 - 6mr_0^8 + 24ml^2r_0^6 -$$

$$12m^2l^2r_0^5 + 12m^2l^4r_0^3 - 64m^3l^6 \;=\; 0\ . \tag{105}$$

Let $r_0 = r_{ISCO}$ be the real solution of the equation (105) which gives the radius of the ISCO of Hayward space-time.

In the limit $l \to 0$, we obtain the radius of ISCO for Schwarzschild black hole which is $r_{ISCO} = 6m$.

4.0.2 Photon orbits:

For null circular geodesics, the effective potential becomes

$$\mathcal{U}_{eff} \;=\; \frac{L^2}{r^2}\mathcal{H}(r) = \frac{L^2}{r^2}\left(1 - \frac{2mr^2}{(r^3 + 2ml^2)}\right) \tag{106}$$

For circular null geodesics at $r = r_c$, we find

$$\mathcal{U}_{eff} \;=\; E^2 \tag{107}$$

and

$$\frac{d\mathcal{U}_{eff}}{dr} \;=\; 0 \tag{108}$$

Thus one may obtain for Hayward space-time, the ratio of energy and angular momentum of the test particle evaluated at $r = r_c$ for circular photon orbits are:

$$\frac{E_c}{L_c} = \pm\sqrt{\frac{1}{r_c^2}\left(1-\frac{2mr_c^2}{(r_c^3+2ml^2)}\right)} \tag{109}$$

and,

$$r_c^6 - 3mr_c^5 + 4ml^2r_c^3 + 4m^2l^4 = 0. \tag{110}$$

Let $D_c = \frac{L_c}{E_c}$ be the impact parameter for null circular geodesics then

$$\frac{1}{D_c} = \frac{E_c}{L_c} = \sqrt{\frac{(r_c^3+2ml^2)-2mr_c^2}{r_c^2(r_c^3+2ml^2)}} \tag{111}$$

Let $r_c = r_{ph}$ be the solution of the equation (110) which gives the radius of the circular photon orbit of the Hayward space-time.

4.1 CM Energy for Hayward space-time:

The components of the four velocity in terms of the energy and angular momentum due to the Killing symmetries of the space-time for time-like particles are

$$u^t = \frac{E}{\mathcal{H}(r)} \tag{112}$$

$$u^r = \pm\sqrt{E^2 - \mathcal{H}(r)\left(1+\frac{L^2}{r^2}\right)} \tag{113}$$

$$u^\theta = 0 \tag{114}$$

$$u^\phi = \frac{L}{r^2}\,. \tag{115}$$

and,

$$u_1^\mu = \left(\frac{E_1}{\mathcal{H}(r)},\ -Z_1,\ 0,\ \frac{L_1}{r^2}\right)\,. \tag{116}$$

$$u_2^\mu = \left(\frac{E_2}{\mathcal{H}(r)},\ -Z_2,\ 0,\ \frac{L_2}{r^2}\right)\,. \tag{117}$$

where

$$Z_1 = \sqrt{E_1^2 - \mathcal{H}(r)\left(1+\frac{L_1^2}{r^2}\right)} \tag{118}$$

$$Z_2 = \sqrt{E_2^2 - \mathcal{H}(r)\left(1+\frac{L_2^2}{r^2}\right)} \tag{119}$$

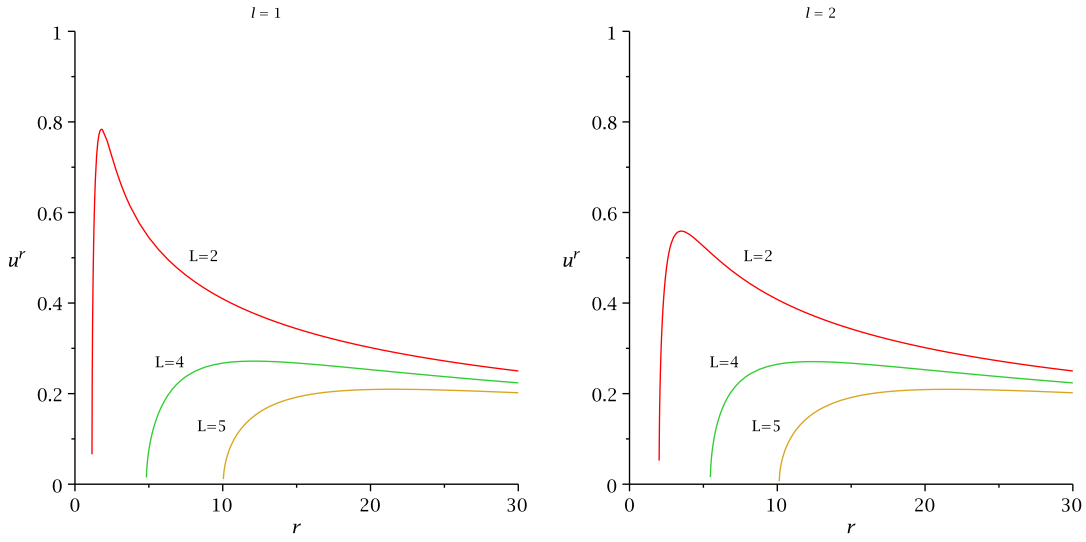

Figure 10: The figure shows the variation of $\dot{r}$ with r for Hayward space-time. Here, $m = 1$.

Substituting this in (30), we find the center of mass energy for Hayward space-time:

$$\left(\frac{E_{cm}}{\sqrt{2}m_0}\right)^2 = 1 + \frac{E_1E_2}{\mathcal{H}(r)} - \frac{Z_1Z_2}{\mathcal{H}(r)} - \frac{L_1L_2}{r^2} \ . \tag{120}$$

Now we can see in the following diagram, the variation of radial velocity and CM energy for Hayward space-time.

Taking, $E_1 = E_2 = 1$ and substituting the value of $\mathcal{H}(r)$, we obtain the CM energy near the event horizon (r_+) of the Hayward space-time:

$$E_{cm}\,|_{r\to r_+} = \sqrt{2}m_0\sqrt{\frac{4r_+^2 + (L_1 - L_2)^2}{2r_+^2}} \ . \tag{121}$$

where r_+ is given in (90).

When we set $r_+ = 2m$, we recover the CM energy of the Schwarzschild black hole:

$$E_{cm} = \sqrt{2}m_0\sqrt{\frac{16m^2 + (L_1 - L_2)^2}{8m^2}} \ . \tag{122}$$

The angular velocity of the Hayward space-time at the r_+ is given by

$$\Omega_H = \frac{\dot{\phi}}{\dot{t}} = \sqrt{\frac{m(r_0^3 - 4ml^2)}{(r_0^3 + 2ml^2)^{\frac{5}{2}}}} \ . \tag{123}$$

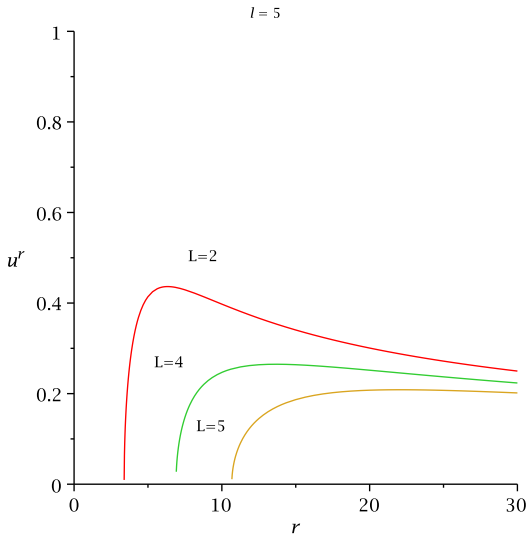

Figure 11: The figure shows the variation of $\dot{r}$ with r for Hayward space-time. Here, $m = 1$.

The critical angular momenta L_i can be written as

$$L_i \;=\; \frac{E_i}{\Omega_H}\,. \tag{124}$$

In the extremal cases, i.e. $27l^2 = 16m^2$, the horizon is at $r_0 = \frac{4}{3}m$ and if one of the values of critical angular momenta diverge we get the infinite amount of CM energy, i.e.

$$E_{cm} \;\longmapsto\; \infty\,. \tag{125}$$

5 Summary and Conclusions:

In this work, we have demonstrated that the collision of two neutral particles falling freely from rest at infinity in the background of the regular black holes. Firstly, we have examined the particle acceleration and collision near the infinite red-shift surface of the Bardeen space-time which is the *first* regular (singularity-free) black hole model in GR. We proved that the center of mass energy is arbitrarily large at the infinite red-shift surface when the black hole is purely extremal. For non-extremal Bardeen black hole, we found that the CM energy is finite and depends upon the critical values of the angular momentum parameter.

Secondly, we have examined the BSW mechanism near the infinite red-shift surface of the ABG black hole which is also a regular black hole space-time and singularity free

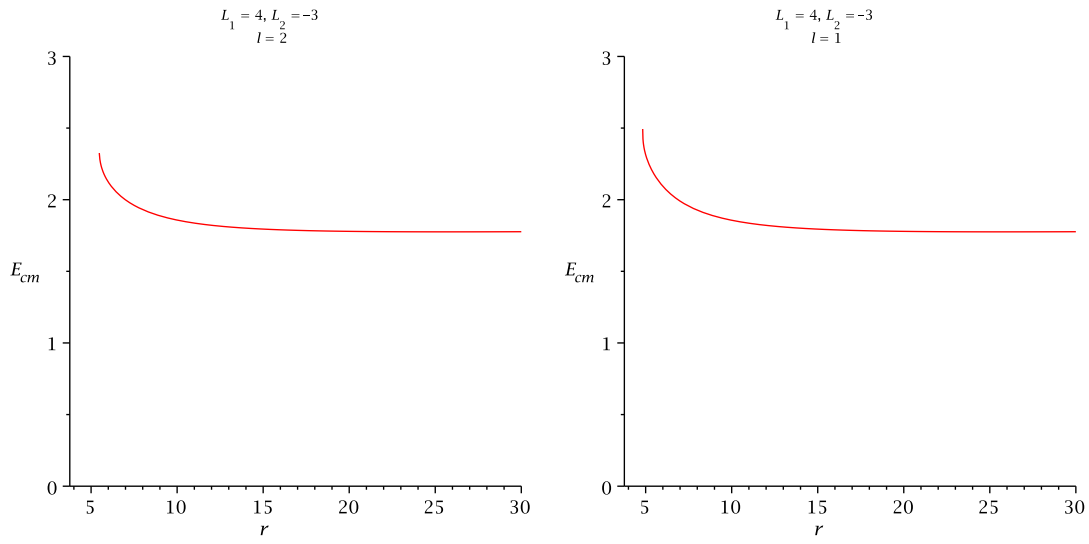

Figure 12: The figure shows the variation of E_{cm} with r for Hayward black hole with different values of angular momentum.

solutions of the coupled system of a non-linear electrodynamics and general relativity. We have showed that the center of mass energy for this black hole also is arbitrarily large at the infinite red-shift surface when it is in the purely extremal situation. For non-extremal ABG black hole, we have seen that the CM energy is finite and depends upon the fine tuning condition of the angular momentum parameter.

Finally, we have tested the BSW mechanism near the infinite red-shift surface of the Hayward black hole which is also a singularity free solution in GR. It is shown that these regular black holes may act as natural particle accelerators with arbitrarily high CM energy when the black hole is precisely extremal.

Moreover, in each cases, we have also studied the properties of equatorial circular geodesic motion by extremization of the effective potential for time-like circular orbits and null circular orbits. We particularly emphasized on the ISCO, MBCO and CPO of these regular black holes. These orbits are useful to extract the information about the back ground geometry and they are also relevant to the astrophysical process.

Our conclusion is that for non-extremal regular space-time the CM energy is finite and depends upon the angular momentum parameter. For extremal regular black holes, the CM energy is unlimited due to the diverging values of the angular momentum parameter of the colliding particles.

References

[1] M. Bañados , J. Silk , and S. M. West, *Phys. Rev. Lett.* **103**, 111102 (2009).

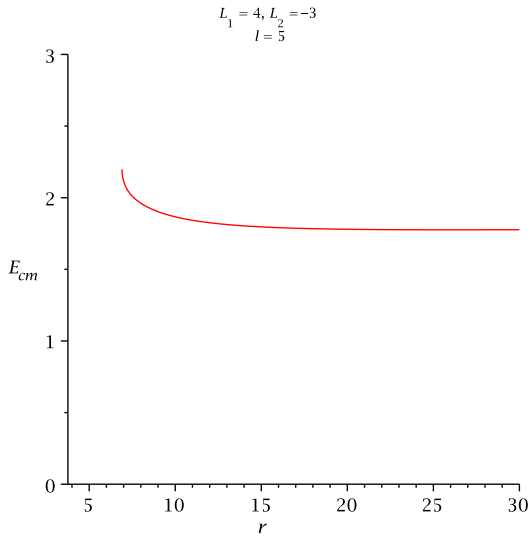

Figure 13: The figure shows the variation of E_{cm} with r for Hayward black hole with different values of angular momentum.

[2] E. Berti , V. Cardoso , L. Gualtieri , F. Pretorius , and U. Sperhake, *Phys. Rev. Lett.* **104**, 239001 (2009).

[3] K. S. Thorn, *Astrophys. J.* **191**, 507 (1974).

[4] T. Jacobson and T. P. Sotiriou, *Phys. Rev. Lett.* **104**, 021101 (2010).

[5] K. Lake, Phys. Rev. Lett. **104**, 211102; **104**, 259903 (2010).

[6] A. Grib , Y. Pavlov, *Astropart. Phys.* **34**, 581 (2011).

[7] A. Grib , Y. Pavlov, *Euro. Phys. Lett.* **101**, 2004 (2013).

[8] T. Harada , M. Kimura, Phys. Rev. D **83**, 024002 (2011).

[9] C. Liu , S. Chen , C. Ding , J. Jing, *Phys. Letters B* **701**, 285-290 (2011).

[10] Y. Li , J. Yang , Y. Li , S. Wei , Y. Liu , *Class. Quantum Gravity* **28**, 225006 (2011).

[11] C. Zhong , S. Gao, *JETP Letters* **94**, 589 (2011).

[12] J. L. Said , K. Z. Adami, Phys. Rev. D **83**, 104047 (2011).

[13] M. Bejger, T. Piran, M. Abramowicz, F. Håkanson, *Phys. Rev. Lett.* **109** 121101 (2012).

[14] S. W. Wei, Y. X. Liu , H. Guo, C. E. Fu , Phys. Rev. D **82**, 103005 (2010).

[15] S. Wei , Y. Liu , H. Li , F. Chen, JHEP **1012**, 066 (2010).

[16] O. Zaslavskii , JETP Lett. **92**, 571 (2010).

[17] Y. Zhu , S. Wu , Y. Jiang , G. Yang , Phys. Rev. D **84**, 123002, 043006 (2011).

[18] I. Hussain, Modern Physics Letters A **27**, 1250068 (2012).

[19] V. P. Frolov, Phys. Rev., **D 86**, 044040 (2012).

[20] M. Sharif , N. Haider, Astrophys Space Sci., DOI: 10.1007/s10509-013-1424-3 (2013).

[21] S. McWilliams , Phys. Rev. Lett., **110**, 011102 (2012).

[22] A. Galajinsky, Phys. Rev. , **D 88**, 027505 (2013).

[23] A. Tursunov , M. Kološ , A. Abdujabbarov , B. Ahmedov and Z. Stuchlík , Phys. Rev., **D 88**, 124001 (2013).

[24] S. Fernando, Gen. Rel. Gravit. **46** 1634 (2014).

[25] M. Patil , P. Joshi , Phys. Rev. D **86**, 044040 (2012).

[26] A. N. Chowdhury , M. Patil , D. Malafarina , P. S. Joshi , Phys. Rev. **D 85**, 104031 (2012).

[27] P. Pradhan, Astrophys Space Sci., DOI: 10.1007/s 10509-014-1896-9 (2014).

[28] J. Bardeen, Conference Proceedings in GR5, Tiflis, U.S.S.R., (1968).

[29] E. Ayón-Beato , A. García , Phys. Rev. Lett. **80**, 5056 (1998).

[30] S. A. Hayward, Phys. Rev. Lett. **96**, 031103 (2006).

[31] E. Ayón-Beato , A. García, Physics Letters **B 493** , 149-152 (2000).

[32] A. Borde, Phys. Rev., **D 55**, 7615 (1997).

[33] S. Ansoldi, Arxiv: 0802.0330 [gr-qc] (2008).

[34] L. Balart, Physics Letters **B 687** 280-285 (2010).

[35] S. Bose, N. Dadhich, Phys. Rev., **D 60**, 064010 (1999).

[36] N. Bretón , Gen. Rel. Gravit. **37(4)** 643-650 (2005).

[37] L. Balart , E. C. Vagenas , Physics Letters **B 730** 14-17 (2014).

[38] A. García , E. Hackman , J. Kunz , C. Lämmerzahl and A. Macias, " Motion of test particles in a regular black hole space-time", arXiv:1306.2549 (2013).

[39] E. F. Eiroa , C. M. Sendra, Classical and Quantum Gravity, **28**(8) 085008 (2011).

[40] S. Zhou , J. Chen, and Y. Wang , International Journal of Modern Physics **D 21**, 1250077 (2011).

[41] S. Chandrashekar , *The Mathematical Theory of Black Holes*, Clarendon Press, Oxford (1983).

[42] J. B. Hartle , *Gravity-An Introduction To Einstein's General Relativity* , Benjamin Cummings (2003).

[43] A. N. Baushev, Int. J. Mod. Phys. D **18**, 1195 (2009).

[44] E. Ayón-Beato, A. García, Physics Letters **B 464**, 25-29 (1999).

[45] E. Ayón-Beato , A. García, Gen. Rel. Gravit. **629**, 31 (1999).

[46] E. Ayón-Beato , A. García, Gen. Rel. Gravit. **635**, 37 (2005).

[47] K. A. Bronnikov , J. C. Fabris, Phys. Rev. Lett. **96**, 251101 (2006).